ACS APPLIED MATERIALS & INTERFACES

Research Article

Cite This: ACS Appl. Mater. Interfaces 2019, 11, 11414−11420

www.acsami.org

Comparative Study of $Mg(CB_{11}H_{12})_2$ and $Mg(TFSI)_2$ at the Magnesium/Electrolyte Interface

Rahul Jay,[†] Anton W. Tomich,[‡] Jian Zhang,[§] Yifan Zhao,[§] Audrey De Gorostiza,[†] Vincent Lavallo,*[,‡] and Juchen Guo*[,†,§]

[†]Department of Chemical and Environmental Engineering, [‡]Department of Chemistry, and [§]Program of Materials Science and Engineering, University of California—Riverside, Riverside, California 92521, United States

Supporting Information

ABSTRACT: An essential requirement for electrolytes in rechargeable magnesium-ion (Mg-ion) batteries is to enable Mg plating−stripping with low overpotential and high Coulombic efficiency. To date, the influence of the Mg/electrolyte interphase on plating and stripping behaviors is still not well understood. In this study, we investigate the Mg/electrolyte interphase from electrolytes based on two Mg salts with weakly coordinating anions: magnesium monocarborane ($Mg(CB_{11}H_{12})_2$) and magnesium bis(trifluoromethanesulfonyl)imide ($Mg(TFSI)_2$). Cyclic voltammetry and chronopotentiometry of Mg plating−stripping demonstrate significantly lower overpotential in the Mg-$(CB_{11}H_{12})_2$ electrolyte than in $Mg(TFSI)_2$ under the same condition. Surface characterizations including X-ray photoelectron spectroscopy and scanning electron microscopy clearly demonstrate the superior chemical and electrochemical stability of the $Mg(CB_{11}H_{12})_2$ electrolyte at the Mg surface without noticeable interphase formation. On the other hand, characterizations of the Mg/electrolyte interface in the $Mg(TFSI)_2$ electrolyte indicate the formation of magnesium oxide, magnesium sulfide, and magnesium fluoride as the interfacial compounds resulting from the decomposition of $TFSI^-$ anions because of both chemical reduction by Mg and cathodic reduction during Mg deposition.

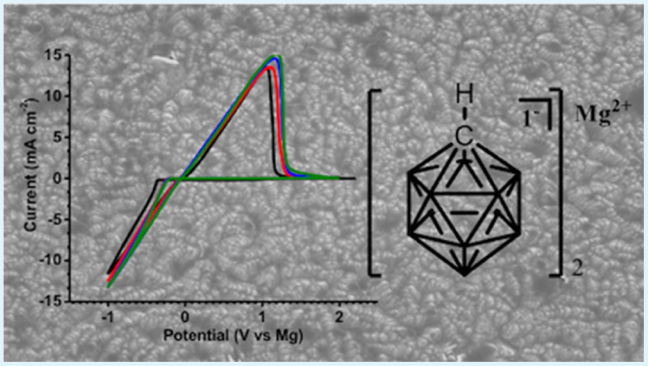

KEYWORDS: *interphase, Mg-ion batteries, Mg metal anode, $Mg(TFSI)_2$, monocarborane*

INTRODUCTION

Rechargeable Mg-ion batteries have received increasing attention as an energy storage technology beyond lithium-ion batteries. However, the development of Mg-ion batteries is hampered by the lack of high-capacity cathode materials and limited options of Mg-ion electrolytes. The conventional Mg-ion electrolytes are mainly based on the organo−haloaluminate complex originating from the seminal works by Gregory et al. in 1990[1] and Aurbach et al. in 2000.[2] These electrolytes typically contain a mixture of Grignard reagents (RMgCl or R_2Mg, R is the alkyl, aryl, or carboranyl group) and Lewis acids (typically $AlCl_3$),[3−7] thus suffering from low anodic stability due to the nucleophilicity of the Grignard reagents.[2,5] Therefore, non-Grignard electrolytes have been developed including the magnesium aluminum chloride complex ($MgCl_2$−$AlCl_3$),[8−12] magnesium alkoxides [ROMgCl or $Mg(OR)_2$],[13,14] fluorinated alkoxides,[15] and amides such as hexamethyldisilazide magnesium chloride (HMDSMgCl)[16] and magnesium bis(hexamethyldisilazide) ($Mg(HMDS)_2$).[17−19] However, a majority of the reported electrolytes still contain active chloride anions, which renders these electrolytes corrosive, thus not compatible with battery components.[18] Therefore, the recent developments are more focused on non-Grignard and halide-free (or the halide sequestered in a polyatomic anion) electrolytes based on Mg salts with weakly coordinating anions including borohydride,[20] hexafluorophosphate,[21] monocarborane ($(CB_{11}H_{12})^-$),[22,23] fluorinated alkoxyborate,[24] and fluorinated alkoxyaluminate anions.[25,26]

Among all the "simple" Mg salts, magnesium bis(trifluoromethanesulfonyl)imide ($Mg(TFSI)_2$) is readily available and soluble in ethers, which are widely considered as the only type of solvents compatible with Mg metal anodes.[27,28] Therefore, its electrochemical properties have been the subject of several investigations. The early studies suggest that Mg could not be deposited from acetonitrile solution of Mg-$(TFSI)_2$ because of the reduction of acetonitrile at a potential of −0.2 V versus Mg,[29] while the ethereal $Mg(TFSI)_2$ solutions seemed capable of reversible Mg plating−stripping, however, with an inferior overpotential.[30−32] The theoretical investigations on $Mg(TFSI)_2$ indicated that the ion pairing between partially reduced Mg^{2+} cations (to Mg^+) and $TFSI^-$, facilitating

Received: January 1, 2019
Accepted: March 12, 2019
Published: March 12, 2019

DOI: 10.1021/acsami.9b00037
ACS Appl. Mater. Interfaces 2019, 11, 11414−11420

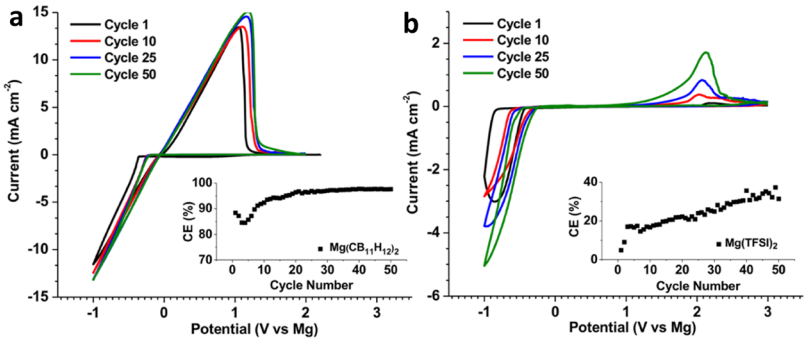

Figure 1. Representative CV scans and CE of Mg plating–stripping in (a) 0.75 M $Mg(CB_{11}H_{12})_2$ and (b) 0.5 M $Mg(TFSI)_2$ in G4 at 50 mV s^{-1} at room temperature.

the cathodic decomposition of $TFSI^-$ anions on the electrode surface.[33] On the contrary, $Mg(CB_{11}H_{12})_2$, developed independently by Tutusaus et al.[22] and McArthur et al.[23] in 2015, was demonstrated as one of the best Mg salts for Mg-ion electrolytes with excellent anodic stability and low plating–stripping overpotential. The opposite electrochemical properties of the $Mg(TFSI)_2$ and $Mg(CB_{11}H_{12})_2$ electrolytes seem to originate from their different interfacial mechanisms. However, the Mg/electrolyte interphase in these electrolytes are not well understood, particularly for $Mg(CB_{11}H_{12})_2$. Therefore, in this study, we aim to obtain the direct information on their interfacial behaviors and interphase compositions through a systematic investigation.

EXPERIMENTAL SECTION

Preparation of Electrolytes. All manipulations were carried out using standard Schlenk or glovebox techniques under a nitrogen or argon atmosphere unless otherwise stated. $Mg(CB_{11}H_{12})_2$ was prepared by the method of McArthur et al.[23] Tetraethylene glycol dimethyl ether (G4) (>99%, Sigma-Aldrich) was distilled over sodium metal under inert conditions on the Schlenk-line and stored with molecular sieves until electrolyte solution was mixed. $Mg(TFSI)_2$ salt (Solvionic, 99.5%) was dried inside a tube furnace at 180 °C under vacuum in an argon (Ar)-filled glovebox for 48 h. The preparation of both electrolytes was conducted inside the Ar-filled glovebox. Water content of G4 and the electrolytes were measured with a Karl Fischer titrator.

Electrochemical Analyses and Material Characterizations. Cyclic voltammetry (CV) and chronopotentiometry of Mg plating–stripping were performed with the three-electrode setup inside the Ar-filled glovebox. The standard platinum working electrode (3 mm disk) was used in the CV experiments. Copper (Cu) foils (Lyon Industries) were used in the Mg deposition experiments. Cu foils were cleaned by soaking in 2.0 M sulfuric acid (Fisher Chemicals) for 3 days. The soaked Cu foils were sonicated three times for 5 min each in anhydrous ethanol (Sigma-Aldrich), and the dried Cu foils were stored in the Ar-filled glovebox for use. Mg foil was used as the electrode in the chemical compatibility study and the Mg-stripping experiments. The Mg foil was polished with 1200 and 2500 grit sand papers inside the glovebox and then washed with anhydrous G4 before use. Scanning electron microscopy (SEM) and energy-dispersive X-ray spectroscopy (EDS) was performed on Nova NanoSEM 450. Samples were carefully washed with G4 and tetrahydrofuran inside the glovebox before being mounted on the sample stubs. To perform X-ray photoelectron spectroscopy (XPS), samples were transferred from the glovebox via sealed stainless steel transfer tubes to the XPS facility. XPS experiments were conducted with Kratos Axis Supra with a dual anode Al/Ag monochromatic X-ray source. The samples were transferred into the analysis chamber via the integrated glovebox filled with inert gas.

RESULTS AND DISCUSSION

Owing to the insolubility of $Mg(CB_{11}H_{12})_2$ in lower glymes, we selected G4 as the solvent for both $Mg(CB_{11}H_{12})_2$ and $Mg(TFSI)_2$. The concentration of the $Mg(TFSI)_2$ electrolyte is 0.5 M, which is close to the highest concentration that can be achieved in G4 at room temperature (Figure S1 in Supporting Information). The concentration of the $Mg(CB_{11}H_{12})_2$ electrolyte is 0.75 M, which is selected for its optimal conductivity as demonstrated by Tutusaus and co-workers.[22] The higher concentration of the $Mg(CB_{11}H_{12})_2$ electrolyte should not fundamentally alter its interfacial mechanism, which is the focus of this study. Indeed, electrochemical analyses indicate that the 0.5 M $Mg(CB_{11}H_{12})_2$ electrolyte demonstrates almost identical behaviors as the 0.75 M electrolyte does in CV, Mg deposition, and chronopotentiometry experiments (Figure S2 in Supporting Information). Figure 1 shows the selected CV cycles of Mg plating–stripping in 0.5 M $Mg(TFSI)_2$ and 0.75 M $Mg(CB_{11}H_{12})_2$ electrolytes at 50 mV s^{-1} with the Pt working electrode, Mg counter electrode, and Mg reference electrode in the three-electrode setup. The Coulombic efficiency (CE) of the plating–stripping process over 50 cycles was calculated from the CV curves and shown as the inset. The water content in both electrolytes was 8 ppm measured with the Karl Fischer titration. The $Mg(CB_{11}H_{12})_2$ electrolyte demonstrates low plating overpotential at −0.5 V versus Mg^{2+}/Mg in the first cycle, which was further lowered to −0.35 V on subsequent cycles. The Mg-stripping potential is at 0 V versus Mg^{2+}/Mg, thus resulting in a small plating–stripping potential hysteresis. On the other hand, although the $Mg(TFSI)_2$ electrolyte indeed displays a pair of reversible redox peaks, corresponding to Mg plating–stripping, the overpotentials are very high: −0.9 V for plating and 2.1 V for stripping versus Mg^{2+}/Mg. Furthermore, the CE of Mg plating–stripping in the $Mg(CB_{11}H_{12})_2$ electrolyte is stabilized at approximately 97% over the course of 50 cycles. In comparison, the CE of Mg plating–stripping in the $Mg(TFSI)_2$ electrolyte is well below 40% during 50 cycles. Despite the different concentration of these two electrolytes, we speculate the significantly different overpotential and CE are due to their different Mg/electrolyte interphase formation mechanisms during the Mg plating–stripping process.

To study the interphase formation during Mg plating, chronopotentiometry depositions (Figure S3 in Supporting Information) were performed in both electrolytes at a current density of 1 mA cm^{-2} for a period of 12 h on a Cu electrode. The X-ray diffraction (XRD) patterns (Figure S4 in Supporting Information) confirm the deposition of Mg metal from both

DOI: 10.1021/acsami.9b00037
ACS Appl. Mater. Interfaces 2019, 11, 11414–11420

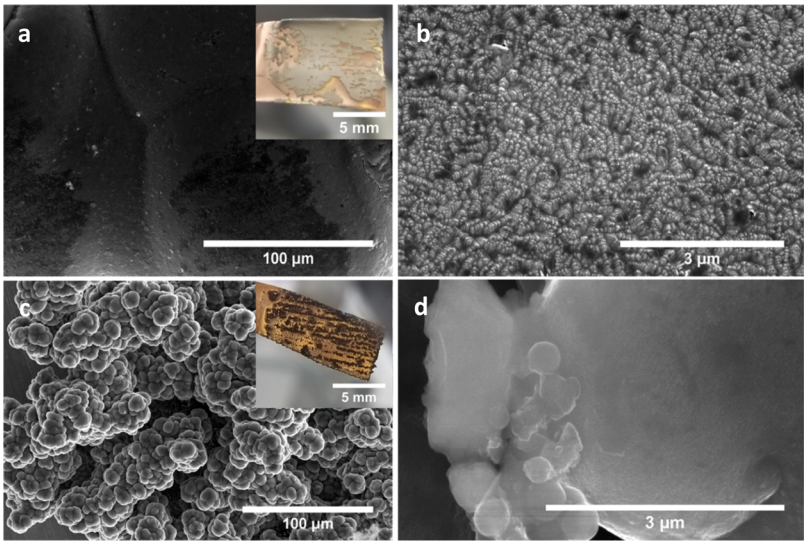

Figure 2. SEM images at different magnifications of Mg deposited on the Cu substrate from (a,b) $Mg(CB_{11}H_{12})_2$ and (c,d) $Mg(TFSI)_2$ electrolytes with constant current at 1 mA cm^{-2} for 12 h at room temperature. Insets are the digital images of Mg deposited on Cu.

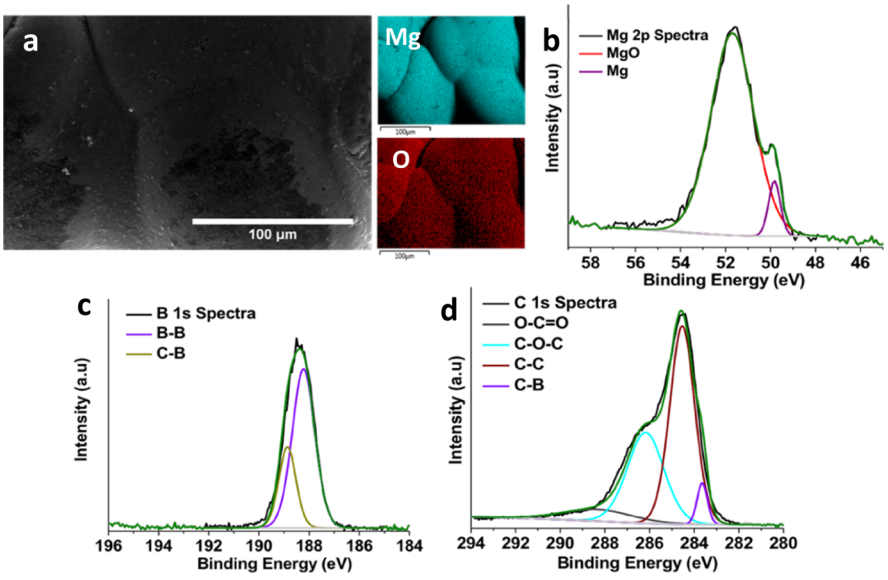

Figure 3. (a) SEM image of Mg deposited from the $Mg(CB_{11}H_{12})_2$ electrolyte with EDS elemental mapping; (b) Mg 2p, (c) B 1s, and (d) C 1s XPS spectra of the deposited Mg surface.

electrolytes. The SEM images in Figure 2a,b at different magnifications display uniform Mg deposition from the $Mg(CB_{11}H_{12})_2$ electrolyte. The digital image inset clearly shows that the deposited Mg metal has a metallic gray color and smooth surface. On the contrary, the Mg deposited from the $Mg(TFSI)_2$ electrolyte has a distinctly different appearance and micromorphology. As depicted in the digital image inset in Figure 2c, the Mg deposited from the $Mg(TFSI)_2$ electrolyte is aggregated black particles on the Cu substrate. The SEM images in Figure 2c,d verify that the Mg deposition from the $Mg(TFSI)_2$ electrolyte indeed is composed by particles instead of smooth deposition. The micromorphology of Mg from the $Mg(TFSI)_2$ electrolyte is consistent with the Mg deposition previously reported by Ha et al. from $Mg(TFSI)_2$ in monoglyme and diglyme.[27]

To understand the stark contrast of Mg deposits from these two electrolytes, EDS and XPS were used to identify the surface composition of the deposited Mg. The EDS elemental mapping of the Mg surface deposited from the $Mg(CB_{11}H_{12})_2$ electrolyte (Figure 3a) displays the strong presence of Mg and oxygen. The corresponding Mg 2p XPS spectrum (Figure 3b) consistently indicates that the Mg-containing species on the surface includes metallic Mg and magnesium oxide (MgO). Considering the absence of oxygen atoms in the $Mg(CB_{11}H_{12})_2$ salt and good resistance of G4 to electrochemical reduction, we believe that the MgO layer is due to the oxidation from the environment. It is also worth noting that the XPS technique only probes a very thin surface layer of a few nanometers. Therefore, the composition ratio shown in the Mg 2p XPS spectrum does not correlate to the actual content of MgO in the deposited Mg. Strong evidence for the stability of the $Mg(CB_{11}H_{12})_2$ electrolyte also comes from the B 1s and C 1s XPS spectra on the Mg surface shown in Figure 3c,d. The B 1s XPS spectrum shows the B−B and B−C bonds, which are consistent with the pristine $Mg(CB_{11}H_{12})_2$ salt (Figure S5 in Supporting Information), resulting from the salt residue on the

DOI: 10.1021/acsami.9b00037
ACS Appl. Mater. Interfaces 2019, 11, 11414−11420

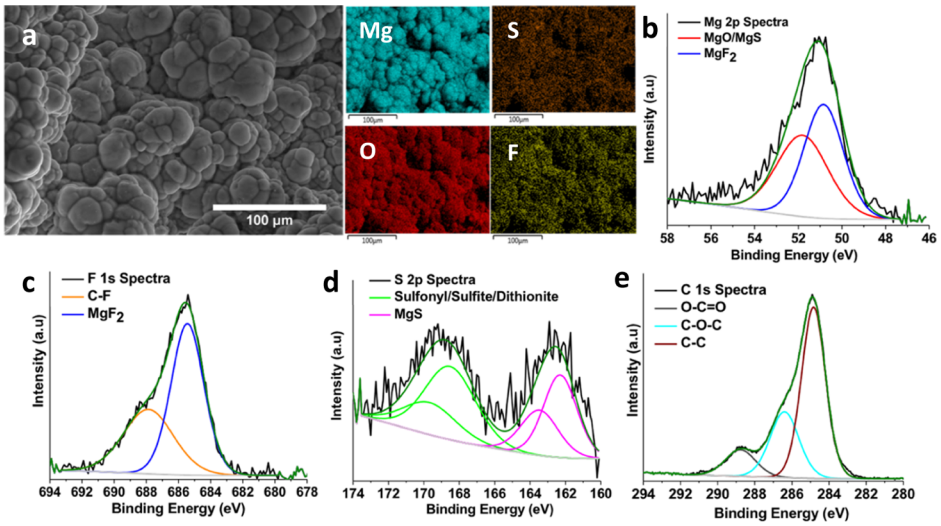

Figure 4. (a) SEM image of Mg deposited from the $Mg(TFSI)_2$ electrolyte with EDS elemental mapping; (b) Mg 2p, (c) F 1s, (d) S 2p, and (e) C 1s XPS spectra of the deposited Mg surface.

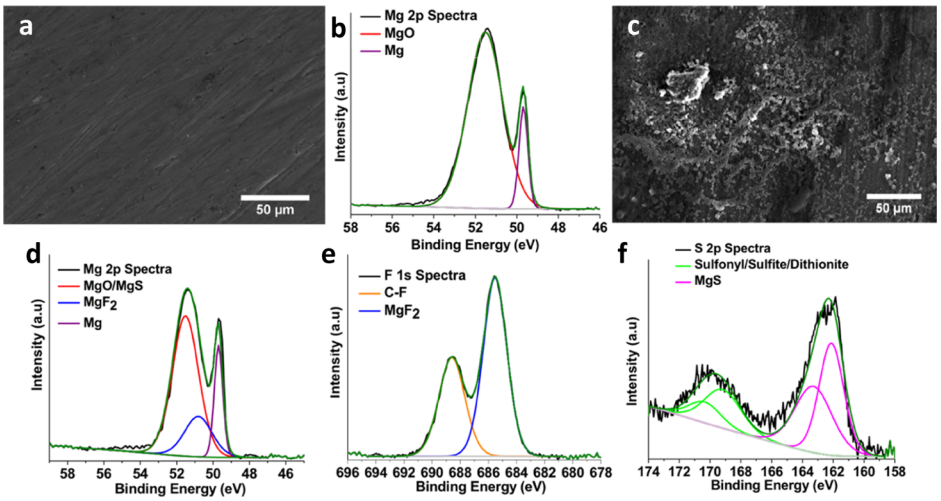

Figure 5. (a) SEM image and (b) Mg 2p XPS spectrum of the Mg surface soaked in the $Mg(CB_{11}H_{12})_2$ electrolyte and (c) SEM image and (d) Mg 2p, (e) F 1s, and (f) S 2p XPS spectra of the Mg surface soaked in the $Mg(TFSI)_2$ electrolyte.

Mg surface. The C 1s XPS spectrum shows the signal from the adventitious carbon (C−C, C−O−C, and O−C═O bonds) from the environmental contamination and the C−B bond from salt residue without indication of G4 decomposition.

In stark contrast to the excellent stability of the $Mg(CB_{11}H_{12})_2$ electrolyte, analyses of the surface of Mg deposited from the $Mg(TFSI)_2$ electrolyte clearly indicate severe passivation layer formation. The EDS elemental mapping in Figure 4a displays surface composition including Mg, oxygen, fluorine, and sulfur. The Mg 2p XPS spectrum in Figure 4b shows Mg bonds from magnesium sulfide (MgS) and MgO (binding energy of Mg in these two compounds are very close) and magnesium fluoride (MgF_2) without indication of metallic Mg. The F 1s XPS spectrum in Figure 4c confirms the existence of MgF_2 and compounds containing C−F bonds on the surface of Mg deposited from $Mg(TFSI)_2$. Similarly, the S 2p XPS spectrum in Figure 4d indicates the existence of MgS and sulfur−oxygen bonds, which can be attributed to the sulfonyl group from the electrolyte residue and/or sulfite (SO_3^{2-}) and dithionite ($S_2O_4^{2-}$) anions from the decomposition of $TFSI^-$ anions.[31,34] The C 1s XPS spectrum in Figure 4e only shows peaks from the adventitious carbon in consistent with the C 1s spectrum from the $Mg(CB_{11}H_{12})_2$ electrolyte, indicating that the G4 solvent is stable.

The EDS and XPS results in Figure 4 lead to the conclusion that the passivation layer is formed during Mg deposition in the $Mg(TFSI)_2$ electrolyte via $TFSI^-$ anion reduction. Rajput et al. through their theoretical investigation[33] proposed that the proneness of $TFSI^-$ anions to reduction is due to a transient ion pair of Mg^+-TFSI^- from partial reduction of Mg^{2+} cations. The proposed electrochemical decomposition mechanism of the $TFSI^-$ anion is shown in the Supporting Information (Scheme S1). Yu et al. proposed that $TFSI^-$ anions could chemically decompose by the nucleophilic attack from the free OH^- anions induced by water content in the electrolyte.[35] It is also known that metallic Mg is capable of reducing C−F, N−S, and S═O bonds,[36,37] thus it is not surprising that the similar decomposition occurs electrochemically for $TFSI^-$ anions. It is unlikely that the monocarborane anion decomposes chemically in the presence of metallic Mg because we prepare the electrolyte in high purity and yield via a Mg reduction. Therefore, to prove that the $TFSI^-$ anion

DOI: 10.1021/acsami.9b00037
ACS Appl. Mater. Interfaces 2019, 11, 11414−11420

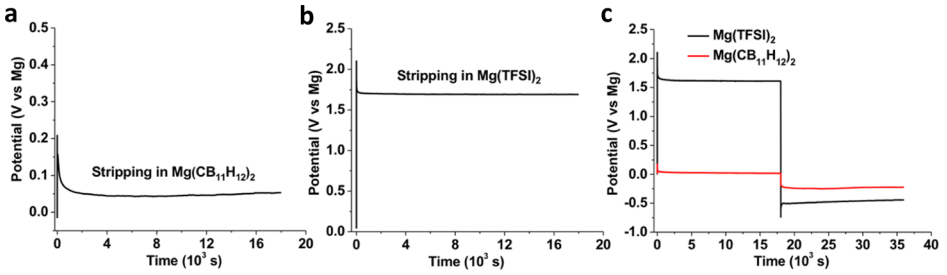

Figure 6. Chronopotentiometry Mg-stripping curve in (a) $Mg(CB_{11}H_{12})_2$ electrolyte and (b) $Mg(TFSI)_2$ electrolyte and (c) chronopotentiometry curves of Mg stripping and plating. The current density is 1 mA cm^{-2} and the duration is 5 h for stripping and 5 h for plating at room temperature.

specifically degrades in the presence of Mg metal anodes and the monocarborane anion does not, we investigated the chemical compatibility of Mg metal in both $Mg(CB_{11}H_{12})_2$ and $Mg(TFSI)_2$ electrolytes. After being soaked in the $Mg(CB_{11}H_{12})_2$ electrolyte for 14 days, no visible change can be observed on the Mg surface (Figure S6 in Supporting Information). Figure 5a displays the SEM image of the soaked Mg surface with no indication of morphology change. The Mg 2p XPS spectrum of the soaked Mg surface (Figure 5b) shows metallic Mg and MgO from the native oxide on the surface. (The native MgO layer cannot be completely removed by polishing as shown in the Mg 2p XPS spectrum of the polished Mg in Figure S6.) The EDS spectrum in Figure S7 (Supporting Information) also evidences no composition change after soaking in the $Mg(CB_{11}H_{12})_2$ electrolyte. On the other hand, the Mg electrode soaked in the $Mg(TFSI)_2$ electrolyte demonstrates visible color change from metal gray to black as shown in Figure S8 in the Supporting Information. Clear surface morphological change (pitting-like) can be observed in the SEM image in Figure 5c. The EDS spectrum in Figure S9 in the Supporting Information clearly shows surface compounds containing significant amounts of O, F, and S elements. The XPS spectra of Mg 2p, F 1s, and S 2p (Figure 5d–f) show very similar results to those on the Mg surface electrochemically deposited from the $Mg(TFSI)_2$ electrolyte. The XPS spectra are strong evidence that $TFSI^-$ anions can be chemically reduced by Mg metal.

The distinctly different chemical stability of $Mg(CB_{11}H_{12})_2$ and $Mg(TFSI)_2$ with Mg metal (i.e., different interfacial compositions) results in very different behaviors of Mg stripping. As shown in Figure 6a,b, the Mg stripping at 1 mA cm^{-2} in the $Mg(CB_{11}H_{12})_2$ electrolyte demonstrates a very low overpotential of 0.05 V versus Mg. On the contrary, the Mg stripping with the same current density in the $Mg(TFSI)_2$ electrolyte demonstrates a significantly higher overpotential at 1.4 V versus Mg. This high overpotential of Mg stripping could contribute to the previous observation that Mg–S two-electrode cells using the $Mg(TFSI)_2$ electrolyte in monoglyme failed to demonstrate discharging capacity.[38,39] The interphase on the Mg electrode also impacts the behavior of Mg plating following the stripping process as displayed in Figure 6c. Mg plating after stripping in the $Mg(CB_{11}H_{12})_2$ electrolyte shows a modest overpotential of −0.25 V versus Mg; on the other hand, Mg plating after stripping in $Mg(TFSI)_2$ shows a high overpotential of −0.5 V versus Mg with a considerably high potential overshoot. The EDS and XPS analysis of the Mg surfaces after stripping and replating (Figures S10–S13 in Supporting Information) show consistent results with the analyses described above: the Mg surface in the $Mg(CB_{11}H_{12})_2$ electrolyte is virtually interphase-free and the one in the $Mg(TFSI)_2$ electrolyte contains oxide, sulfide, and fluoride compounds.

CONCLUSIONS

Through systematic electrochemical analyses and microscopic and spectroscopic characterizations, we have demonstrated superior Mg plating–stripping performance of the $Mg(CB_{11}H_{12})_2$ electrolyte in comparison with $Mg(TFSI)_2$. Such excellent electrochemical performance of $Mg(CB_{11}H_{12})_2$ can be unambiguously attributed to the superb chemical and electrochemical stability at the Mg/electrolyte interface. Our results indicate that virtually, no interphase formation occurs during Mg plating because of the cathodic stability of the $(CB_{11}H_{12})^-$ anion. On the contrary, we also demonstrate that $Mg(TFSI)_2$ is an inferior salt for the Mg-ion electrolyte because of its severe passivation layer formation, which occurs both chemically and electrochemically due to the reduction of the $TFSI^-$ anion. $Mg(TFSI)_2$ may only be a feasible salt for Mg-ion electrolytes with proper Mg anode protection as demonstrated by Ban and co-workers.[40] Undoubtedly, $Mg(CB_{11}H_{12})_2$ is one of the most Mg-compatible salts for Mg-ion electrolytes to date.

ASSOCIATED CONTENT

Supporting Information

The Supporting Information is available free of charge on the ACS Publications website at DOI: 10.1021/acsami.9b00037.

Image of 0.6 M $Mg(TFSI)_2$ solution in G4 without complete dissolution; CV curves, SEM images of Mg deposited on Cu, and Mg stripping–plating curves from the 0.5 M $Mg(CB_{11}H_{12})_2$ electrolyte; chronopotentiometry curves of Mg deposition on Cu from $Mg(CB_{11}H_{12})_2$ and $Mg(TFSI)_2$ electrolytes; XRD patterns of the deposited Mg; B 1s XPS spectrum of the $Mg(CB_{11}H_{12})_2$ salt; proposed mechanism of cathodic decomposition of the $TFSI^-$ anion; digital images of polished Mg electrodes; digital images and EDS and XPS spectra of Mg electrodes soaked in $Mg(CB_{11}H_{12})_2$ and $Mg(TFSI)_2$ electrolytes; EDS and XPS spectra of Mg electrodes after stripping in $Mg(CB_{11}H_{12})_2$ and $Mg(TFSI)_2$ electrolytes; and EDS and XPS spectra of Mg electrodes after plating, following stripping in $Mg(CB_{11}H_{12})_2$ and $Mg(TFSI)_2$ electrolytes (PDF)

AUTHOR INFORMATION

Corresponding Authors

*E-mail: vincent.lavallo@ucr.edu (V.L.).
*E-mail: jguo@engr.ucr.edu (J.G.).

DOI: 10.1021/acsami.9b00037
ACS Appl. Mater. Interfaces 2019, 11, 11414–11420

ORCID

Jian Zhang: 0000-0003-0356-7611
Vincent Lavallo: 0000-0001-8945-3038
Juchen Guo: 0000-0001-9829-1202

Funding

National Science Foundation: DMR-1508537.

Notes

The authors declare no competing financial interest.

■ ACKNOWLEDGMENTS

The authors gratefully acknowledge the support from the National Science Foundation (DMR-1508537). XPS work was performed at the UC Irvine Materials Research Institute (IMRI) instrumentation funded in part by the National Science Foundation Major Research Instrumentation Program under grant no. CHE-1338173.

■ REFERENCES

(1) Gregory, T. D.; Hoffman, R. J.; Winterton, R. C. Nonaqueous Electrochemistry of Magnesium: Applications to Energy Storage. *J. Electrochem. Soc.* **1990**, *137*, 775−780.
(2) Aurbach, D.; Lu, Z.; Schechter, A.; Gofer, Y.; Gizbar, H.; Turgeman, R.; Cohen, Y.; Moshkovich, M.; Levi, E. Prototype Systems for Rechargeable Magnesium Batteries. *Nature* **2000**, *407*, 724−727.
(3) Aurbach, D.; Schechter, A.; Moshkovich, M.; Cohen, Y. On the Mechanisms of Reversible Magnesium Deposition Processes. *J. Electrochem. Soc.* **2001**, *148*, A1004−A1014.
(4) Aurbach, D.; Cohen, Y.; Moshkovich, M. The Study of Reversible Magnesium Deposition by In Situ Scanning Tunneling Microscopy. *Electrochem. Solid-State Lett.* **2001**, *4*, A113−A116.
(5) Lv, D.; Xu, T.; Saha, P.; Datta, M. K.; Gordin, M. L.; Manivannan, A.; Kumta, P. N.; Wang, D. A Scientific Study of Current Collectors for Mg Batteries in $Mg(AlCl_2EtBu)_2$/THF Electrolyte. *J. Electrochem. Soc.* **2013**, *160*, A351−A355.
(6) Aurbach, D.; Gofer, Y.; Lu, Z.; Schechter, A.; Chusid, O.; Gizbar, H.; Cohen, Y.; Ashkenazi, V.; Moshkovich, M.; Turgeman, R.; Levi, E. A Short Review on the Comparison between Li Battery Systems and Rechargeable Magnesium Battery Technology. *J. Power Sources* **2001**, *97*−*98*, 28−32.
(7) Aurbach, D.; Gizbar, H.; Schechter, A.; Chusid, O.; Gottlieb, H. E.; Gofer, Y.; Goldberg, I. Electrolyte Solutions for Rechargeable Magnesium Batteries Based on Organomagnesium Chloroaluminate Complexes. *J. Electrochem. Soc.* **2002**, *149*, A115−A121.
(8) Liu, T.; Cox, J. T.; Hu, D.; Deng, X.; Hu, J.; Hu, M. Y.; Xiao, J.; Shao, Y.; Tang, K.; Liu, J. A Fundamental Study on the $[(\mu\text{-}Cl)_3Mg_2(THF)_6]^+$ Dimer Electrolytes for Rechargeable Mg Batteries. *Chem. Commun.* **2015**, *51*, 2312−2315.
(9) Liu, T.; Shao, Y.; Li, G.; Gu, M.; Hu, J.; Xu, S.; Nie, Z.; Chen, X.; Wang, C.; Liu, J. A Facile Approach Using $MgCl_2$ to Formulate High Performance Mg^{2+} Electrolytes for Rechargeable Mg Batteries. *J. Mater. Chem. A* **2014**, *2*, 3430−3438.
(10) Barile, C. J.; Barile, E. C.; Zavadil, K. R.; Nuzzo, R. G.; Gewirth, A. A. Electrolytic Conditioning of a Magnesium Aluminum Chloride Complex for Reversible Magnesium Deposition. *J. Phys. Chem. C* **2014**, *118*, 27623−27630.
(11) Canepa, P.; Jayaraman, S.; Cheng, L.; Rajput, N. N.; Richards, W. D.; Gautam, G. S.; Curtiss, L. A.; Persson, K. A.; Ceder, G. Elucidating the Structure of the Magnesium Aluminum Chloride Complex Electrolyte for Magnesium-Ion Batteries. *Energy Environ. Sci.* **2015**, *8*, 3718−3730.
(12) Doe, R. E.; Han, R.; Hwang, J.; Gmitter, A. J.; Shterenberg, I.; Yoo, H. D.; Pour, N.; Aurbach, D. Novel, electrolyte solutions comprising fully inorganic salts with high anodic stability for rechargeable magnesium batteries. *Chem. Commun.* **2014**, *50*, 243−245.
(13) Wang, F.-f.; Guo, Y.-s.; Yang, J.; Nuli, Y.; Hirano, S.-i. A Novel Electrolyte System without a Grignard Reagent for Rechargeable Magnesium Batteries. *Chem. Commun.* **2012**, *48*, 10763−10765.
(14) Nelson, E. G.; Kampf, J. W.; Bartlett, B. M. Enhanced Oxidative Stability of Non-Grignard Magnesium Electrolytes through Ligand Modification. *Chem. Commun.* **2014**, *50*, 5193−5195.
(15) Crowe, A. J.; Stringham, K. K.; Bartlett, B. M. Fluorinated Alkoxide-Based Magnesium-Ion Battery Electrolytes That Demonstrate Li-Ion-Battery-like High Anodic Stability and Solution Conductivity. *ACS Appl. Mater. Interfaces* **2016**, *8*, 23060−23065.
(16) Liao, C.; Sa, N.; Key, B.; Burrell, A. K.; Cheng, L.; Curtiss, L. A.; Vaughey, J. T.; Woo, J.-J.; Hu, L.; Pan, B.; Zhang, Z. The Unexpected Discovery of the $Mg(HMDS)_2/MgCl_2$ Complex as a Magnesium Electrolyte for Rechargeable Magnesium Batteries. *J. Mater. Chem. A* **2015**, *3*, 6082−6087.
(17) Kim, H. S.; Arthur, T. S.; Allred, G. D.; Zajicek, J.; Newman, J. G.; Rodnyansky, A. E.; Oliver, A. G.; Boggess, W. C.; Muldoon, J. Structure and Compatibility of a Magnesium Electrolyte with a Sulphur Cathode. *Nat. Commun.* **2011**, *2*, 427.
(18) Zhao-Karger, Z.; Zhao, X.; Fuhr, O.; Fichtner, M. Bisamide Based Non-Nucleophilic Electrolytes for Rechargeable Magnesium Batteries. *RSC Adv.* **2013**, *3*, 16330−16335.
(19) Merrill, L. C.; Schaefer, J. L. Conditioning-Free Electrolytes for Magnesium Batteries Using Sufone-Ether Mixtures with Increased Thermal Stability. *Chem. Mater.* **2018**, *30*, 3971−3974.
(20) Mohtadi, R.; Matsui, M.; Arthur, T. S.; Hwang, S.-J. Magnesium Borohydride: From Hydrogen Storage to Magnesium Battery. *Angew. Chem., Int. Ed.* **2012**, *51*, 9780−9783.
(21) Keyzer, E. N.; Glass, H. F. J.; Liu, Z.; Bayley, P. M.; Dutton, S. E.; Grey, C. P.; Wright, D. S. $Mg(PF_6)_2$-Based Electrolyte Systems: Understanding Electrolyte-Electrode Interactions for the Development of Mg-Ion Batteries. *J. Am. Chem. Soc.* **2016**, *138*, 8682−8685.
(22) Tutusaus, O.; Mohtadi, R.; Arthur, T. S.; Mizuno, F.; Nelson, E. G.; Sevryugina, Y. V. An Efficient Halogen-Free Electrolyte for Use in Rechargeable Magnesium Batteries. *Angew. Chem., Int. Ed.* **2015**, *54*, 7900−7904.
(23) McArthur, S. G.; Geng, L.; Guo, J.; Lavallo, V. Cation Reduction and Comproportionation as Novel Strategies to Produce High Voltage, Halide Free, Carborane Based Electrolytes for Rechargeable Mg Batteries. *Inorg. Chem. Front.* **2015**, *2*, 1101−1104.
(24) Zhao-Karger, Z.; Gil Bardaji, M. E.; Fuhr, O.; Fichtner, M. A New Class of Non-Corrosive, Highly Efficient Electrolytes for Rechargeable Magnesium Batteries. *J. Mater. Chem. A* **2017**, *5*, 10815−10820.
(25) Herb, J. T.; Nist-Lund, C. A.; Arnold, C. B. A Fluorinated Alkoxyaluminate Electrolyte for Magnesium-Ion Batteries. *ACS Energy Lett.* **2016**, *1*, 1227−1232.
(26) Herb, J. T.; Nist-Lund, C. A.; Arnold, C. B. A Fluorinated Dialkoxide-Based Magnesium-Ion Electrolyte. *J. Mater. Chem. A* **2017**, *5*, 7801−7805.
(27) Ha, S.-Y.; Lee, Y.-W.; Woo, S. W.; Koo, B.; Kim, J.-S.; Cho, J.; Lee, K. T.; Choi, N.-S. Magnesium(II) Bis(trifluoromethane sulfonyl) imide-based Electrolytes with Wide Electrochemical Windows for Rechargeable Magnesium Batteries. *ACS Appl. Mater. Interfaces* **2014**, *6*, 4063−4073.
(28) Ma, Z.; Kar, M.; Xiao, C.; Forsyth, M.; MacFarlane, D. R. Electrochemical Cycling of Mg in $Mg[TFSI]_2$/Tetraglyme Rlectrolytes. *Electrochem. Commun.* **2017**, *78*, 29−32.
(29) Tran, T. T.; Lamanna, W. M.; Obrovac, M. N. Evaluation of $Mg[N(SO_2CF_3)_2]_2$/Acetonitrile Electrolyte for Use in Mg-Ion Cells. *J. Electrochem. Soc.* **2012**, *159*, A2005−A2009.
(30) Fukutsuka, T.; Asaka, K.; Inoo, A.; Yasui, R.; Miyazaki, K.; Abe, T.; Nishio, K.; Uchimoto, Y. New Magnesium-Ion Conductive Electrolyte Solution Based on Triglyme for Reversible Magnesium Metal Deposition and Dissolution at Ambient Temperature. *Chem. Lett.* **2014**, *43*, 1788−1790.
(31) Shterenberg, I.; Salama, M.; Yoo, H. D.; Gofer, Y.; Park, J.-B.; Sun, Y.-K.; Aurbach, D. Evaluation of $(CF_3SO_2)_2N^-$ (TFSI) Based

DOI: 10.1021/acsami.9b00037
ACS Appl. Mater. Interfaces 2019, 11, 11414−11420

Electrolyte Solutions for Mg Batteries. *J. Electrochem. Soc.* **2015**, *162*, A7118−A7128.
(32) Terada, S.; Mandai, T.; Suzuki, S.; Tsuzuki, S.; Watanabe, K.; Kamei, Y.; Ueno, K.; Dokko, K.; Watanabe, M. Thermal and Electrochemical Stability of Tetraglyme-Magnesium Bis-(trifluoromethanesulfonyl)amide Complex: Electric Field Effect of Divalent Cation on Solvate Stability. *J. Phys. Chem. C* **2016**, *120*, 1353−1365.
(33) Rajput, N. N.; Qu, X.; Sa, N.; Burrell, A. K.; Persson, K. A. The Coupling Between Stability and Ion Pair Formation in Magnesium Electrolytes from First-Principles Quantum Mechanics and Classical Molecular Dynamics. *J. Am. Chem. Soc.* **2015**, *137*, 3411−3420.
(34) Parimalam, B. S.; Lucht, B. L. Reduction Reactions of Electrolyte Salts for Lithium Ion Batteries: $LiPF_6$, $LiBF_4$, LiDFOB, LiBOB, and LiTFSI. *J. Electrochem. Soc.* **2018**, *165*, A251−A255.
(35) Yu, Y.; Baskin, A.; Valero-Vidal, C.; Hahn, N. T.; Liu, Q.; Zavadil, K. R.; Eichhorn, B. W.; Prendergast, D.; Crumlin, E. J. Instability at the Electrode/Electrolyte Interface Induced by Hard Cation Chelation and Nucleophilic Attack. *Chem. Mater.* **2017**, *29*, 8504−8512.
(36) Hu, J.; Zhao, Y.; Ni, C.; Hu, J. Magnesium Metal-Mediated Reductive Trifluoromethylation of Aldehydes with Phenyl Trifluoromethyl Sulfone. *Synthesis* **2010**, *11*, 1899−1904.
(37) Kiplinger, J. L.; Richmond, T. G.; Osterberg, C. E. Activation of Carbon-Fluorine Bonds by Metal Complexes. *Chem. Rev.* **1994**, *94*, 373−431.
(38) Li, X.; Gao, T.; Han, F.; Ma, Z.; Fan, X.; Hou, S.; Eidson, N.; Li, W.; Wang, C. Reducing Mg Anode Overpotential via Ion Conductive Surface Layer Formation by Iodine Additive. *Adv. Energy Mater.* **2018**, *8*, 1701728.
(39) Gao, T.; Ji, X.; Hou, S.; Fan, X.; Li, X.; Yang, C.; Han, F.; Wang, F.; Jiang, J.; Xu, K.; Wang, C. Thermodynamics and Kinetics of Sulfur Cathode during Discharge in $MgTFSI_2$−DME Electrolyte. *Adv. Mater.* **2018**, *30*, 1704313.
(40) Son, S.-B.; Gao, T.; Harvey, S. P.; Steirer, K. X.; Stokes, A.; Norman, A.; Wang, C.; Cresce, A.; Xu, K.; Ban, C. An Artificial Interphase Enables Reversible Magnesium Chemistry in Carbonate Electrolytes. *Nat. Chem.* **2018**, *10*, 532−539.

DOI: 10.1021/acsami.9b00037
ACS Appl. Mater. Interfaces 2019, 11, 11414−11420